Computational Study on the Effects of Gravity Load on OoP Inter Storey Drift Approach of URM Infilled RC Frame

Conference Paper · September 2018

5 authors, including:

Filip Anić
Josip Juraj Stossmayer University of Osijek

Davorin Penava
Josip Jurar Strossmayer University of Osijek

Vasilis Sarhosis
University of Leeds

Lars Abrahamczyk
Bauhaus Universität Weimar

9th International Congress of Croatian Society of Mechanics
18-22 September 2018
Split, Croatia

Computational Study on the Effects of Gravity Load on OoP Inter Storey Drift Approach of URM Infilled RC Frame

Filip ANIĆ*, Davorin PENAVA*, Silva LOZANČIĆ*, Vasilis SARHOSIS+, Lars ABRAHAMCZYK†

**** Josip Juraj Strossmayer University of Osijek, Faculty of Civil Engineering Osijek, 3 Vladimir Prelog Street, HR-31000 Osijek, Croatia***
E-mails: {filip.anic, davorin.penava, silva.lozancic}@gfos.hr

+Bauhaus-Universität Weimar, Earthquake Damage Analysis Center, Marienstraße 7A, D-99421 Weimar, Germany
E-mail: lars.abrahamczyk @uni-weimar.de

†Newcastle University, School of Engineering, 1 Science Square, NE4 5TG, Newcastle upon Tyne, United Kingdom
E-mail: vasilis.sarhosis@ncl.ac.uk

***Abstract**. This paper presents a study on effects of gravity load on OoP behaviour of RC frames with URM infill panels. The study was carried out on a 3D FE micromodel using inter – storey drift approach. Six distinct models were observed for each case, i.e. with and without the gravity load. Models differ in account of having / not having infill and various types of openings (different sizes and positions). From the results analysis, high agreeance with other experimental studies was found. Also, it was found that two approaches differ greatly. Without the gravity load, the infill developed negligible stresses and arching action was not detected. On the contrary, with the gravity load the infill obtained greater stresses, damage and two-hinged arching action was detected. In both cases, the initial stiffness was not affected by the infill or the opening. Infill and openings did modify the post peak behaviour in the case of models with gravity loads.*

1 Introduction

Masonry infill walls are excited laterally both in in-plane (IP) and out-of-plane (OoP) direction during seismic action. Yet, the common practice is to evaluate IP and OoP behavior separately. The majority of OoP studies are conducted with inertial force approach, mostly by loading the infill with airbag [1]–[3]. Fewer studies [4], [5] were done with inter-storey drift ratio approach, where the frame is loaded rather than the infill. The truth is certainly somewhere in between the two approaches. One of the main outcomes of the findings is that arching action develops as discovered by [6]. Arching action was found beneficial as it rises the lateral resistance of walls.

This paper presents studies on OoP inter-storey drift acted upon RC frame with unreinforced masonry wall (URM) containing openings - positioned centrically and eccentrically (Tab. 1). The study also includes the influence of columns gravity, i.e. gravity load. With the infills inertial approach, the gravity load produced degradation of infills stiffness and different crack patterns [7]. Yet, the effect of gravity load is still

unknown with inter-storey drift approach. Although, from simple mechanics, one can foresee that it will certainly influence the initial stiffness.
The study was conducted with Atena 3D software [8].

Table 1: Specimens considered

Model Mark	Appearance of the specimen	Opening	
		Type and area	Position
CD	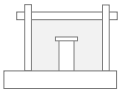	Door l_o / h_o = 0.35 / 0.90 m A_o = 0.32 m^2 A_o / A_i = 0.14	Centric $e_o = l_i / 2$ = 0.90 m
CW	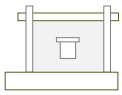	Window l_o / h_o = 50.0 / 60.0 cm A_o = 0.30 m^2 A_o / A_i = 0.13	Centric $e_o = l_i / 2$ = 0.90 m P = 0.40 m
ED	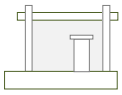	Door l_o / h_o = 0.35 / 0.90 m A_o = 0.32 m^2 A_o / A_i = 0.14	Eccentric $e_o = h_i / 5 + l_o / 2$ = 0.44 m
EW	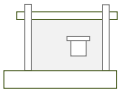	Window l_o / h_o = 50.0 / 60.0 cm A_o = 0.30 m^2 A_o / A_i = 0.13	Eccentric $e_o = h_i / 5 + l_o / 2$ = 0.44 m P = 0.40 m
BF	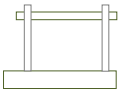	Bare frame	
FI	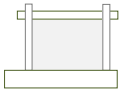	Full infill	

2 Material and methods

2.1 Numerical materials

Numerical materials were adopted from validated 2D IP micromodel from [9]. The materials were additionally modified to accommodate 3D effects and infills OoP behaviour. The cyclic, quasi – static IP 3D BF model was calibrated based on experimental results by [10]. Likewise, BF model can be considered calibrated in OoP direction. Infills OoP behaviour was calibrated on a wall micromodel tested by 4 – point

OoP bending test as given by EN 1052-2 [11] provisions. Concrete frame, lintel and block have CC Nonlinear Cementitious 2 [12] material model (Tab.2). Interface properties are shown in Table 4. Reinforcement material model is presented in Table 3.

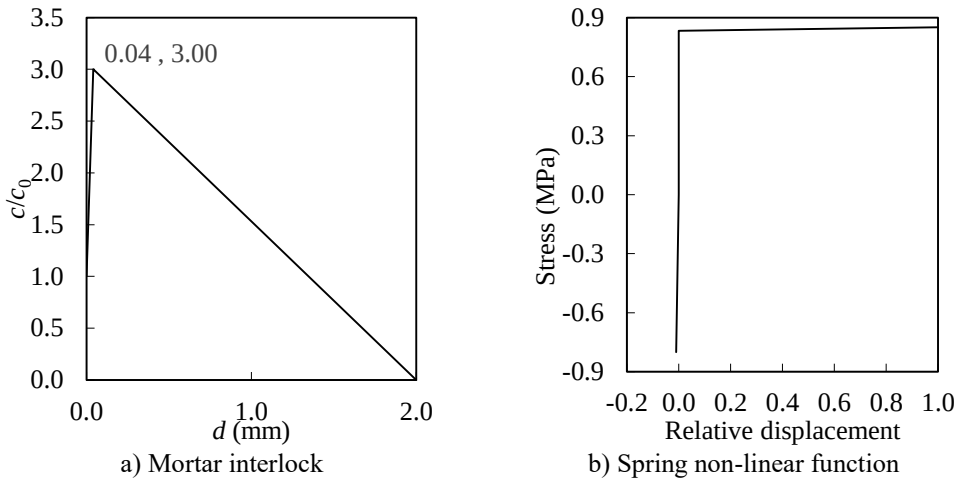

Figure 1: Material functions

Table 2: Non-linear cementitious 2 material properties for each constituent

Description		Frame concrete	Concrete lintel	Clay block	Unit
Elastic modulus	E	4.100 E+04	3.032 E+04	5.650 E+03	MPa
Poisson's ratio	μ	0.200	0.200	0.100	/
Tensile strength	f_t	4.000	2.317	1.800	MPa
Compressive strength	f_c	-5.800 E+01	-2.550 E+01	-1.750 E+01	MPa
Specific fracture energy	G_f	1.200 E-04	5.739 E-05	4.500 E-04	MN/m
Crack spacing	s_{max}	0.125	0.125	-5.000 E-04	m
Tensile stiffening	c_{ts}	0.400	0.400	-1.358 E-03	/
Critical compressive disp.	W_d	-1.010 E-03	-5.000 E-04	-5.000 E-04	/
Plastic strain at f_c	ε_{cp}	-1.417 E-03	-8.411 E-04	-1,358 E-03	/
Reduction of f_c due to cracks	$r_{c.lim}$	0.800	0.800	0.800	/
Crack shear stiffness factor	S_F	20.000	20.000	20.000	/
Direction of plastic flow	β	-0.100	0.000	0.000	
Aggregate size		1.600 E-02	2.000 E-02	/	m
Fixed crack model coefficient		1.000	1.000	1.000	/

Table 3: Bilinear steel reinforcement material properties

Description	Symbol	Value	Unit
Elastic modulus	E	2.10 E+05	MPa
Yield strength	σ_y	5.50 E+02	MPa
Tensile strength	σ_t	6.50 E+02	MPa
Limited ductility of steel	ε_{lim}	0.01	/

Table 4: Interface material properties

Description	Symbol	Mortar bedjoint	Mortar headjoint	Unit
		Value	Value	
Normal stiffness	K_{nn}	5.65 E+05	8.50 E+04	MN/m^2
Min. normal stiffness	$K_{nn.min}$	5.65 E+02	8.50 E+01	MN/m^2
Tangential stiffness	K_{tt}	2.57 E+05	3.86 E+04	MN/m^2
Min. tangential stiffness	$K_{tt.min}$	2.57 E+02	3.86 E+01	MN/m^2
Tensile strength	f_t	0.20	0.20	MPa
Cohesion	c	0.35	0.35	MPa
Friction coefficient		0.24	0.24	/
Interlock function		see Fig. 1a	/	

2.2 Numerical model

The numerical model is assembled from 3D, 2D and 1D constituents. Solid, 3D constituents are used to model concrete frame and lintel, as well as clay blocks. 2D elements designate mortar interface on contacts, while 1D constituents represent reinforcement and are modelled as truss elements. The rebar has perfect connection to the surrounding concrete.

Regarding boundary conditions, models differ greatly (Fig.3). On one hand, model with the gravity load (Fig.3a) had additional vertical force, column supports and nonlinear (NL) spring in y direction. On the other hand, model without gravity load contains only prescribed deformation and foundation support. The loading protocol for the model with gravity load can be divided into two commands: 1. Firstly, gravity load of 365 kN in applied in 5 steps; 2. When the force is applied, column supports in x and z direction are activated and prescribed deformation of δ = 0.1 mm / step is activated. Foundation and NL spring is active at all times.

The NL spring with properties shown in Figure 1b represents friction forces due to large gravity load on column. For more details about the spring, please refer to [13] paper.

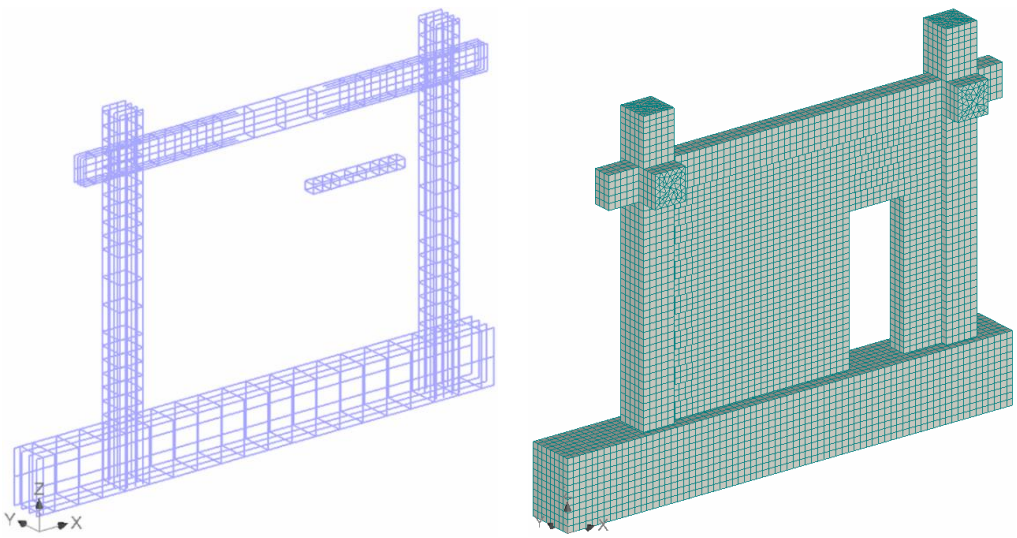

a) Reinforcement b) FE mesh of 4 cm

Figure 2: FE model on ED specimen example

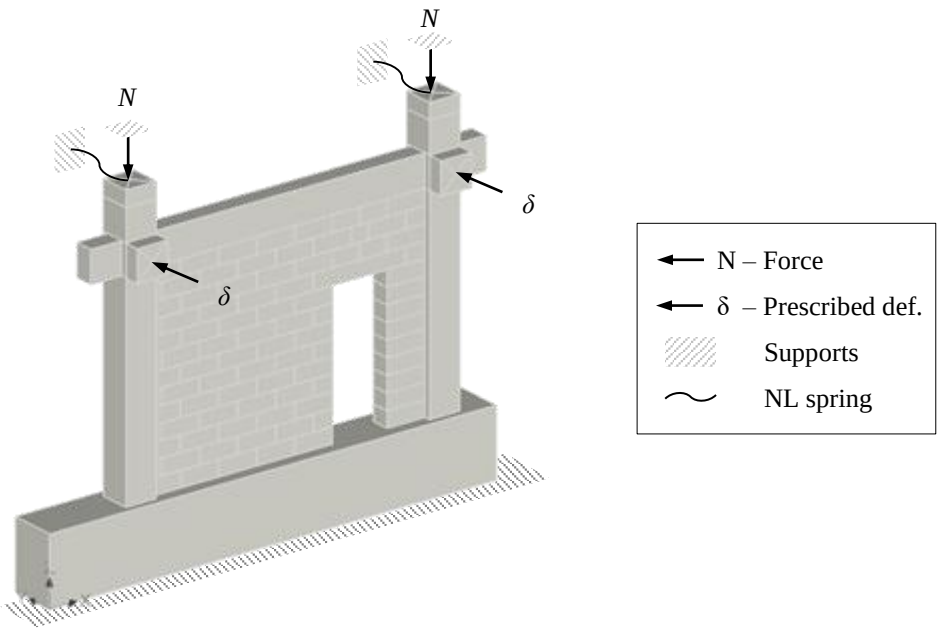

a) Boundary condition with gravity load

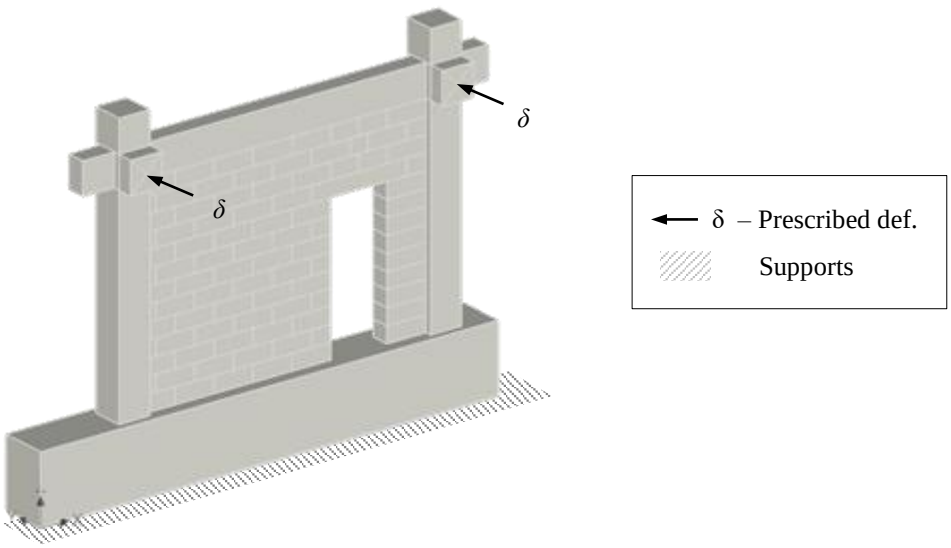

b) Boundary condition without gravity load

Figure 3: Boundary conditions

3 Results

Results are presented for both models with and without the gravity load, for front, back and side view. Front view is designated as side where the load is applied.

Displacements in *y* direction on ED model without gravity load is shown on Figure 4.

Force versus displacement relations are shown on Figure 5, where primary horizontal axis denotes displacements *d*, while primary vertical axis denotes cumulative OoP force from both columns *W*. Secondary horizontal axis plots inter-storey drift ratios d_r, and secondary vertical axis differences from maximal forces of BF model V_{max}.

Crack patterns at maximum displacement are displayed on Figure 6 & 7. The minimum crack with was set to hairline as indication of slight or moderate damage to the infill by FEMA 306 [14].

Minimal principal stresses of the frame at maximal force are plotted on Figures 8 & 9. In the case of model without the gravity load (Fig.9) maximal force is located at maximal displacement. Correspondingly, minimal principal stresses of the infill at maximal force are plotted on Figures 10 & 11.

4 Discussions and conclusions

A 3D FE model of RC frame with URM infill was modelled in order to evaluate the effects of gravity load on inter-storey drift ratio approach. BF model can be considered calibrated in OoP direction as it was calibrated in IP direction. The OoP properties of URM walls were calibrated on micromodels that mirror the conducted 4 – point OoP bending experiments.

From Figures 4 - 11, it can be concluded that:

1) In both cases with and without gravity load, the highest displacement occurred at the top of the column and lowest at the bottom. Same was observed on shaking table test done by [15]. Also, the rotation of the beam can be observed in both models. The rotation, i.e. torsion of the beam resulted in losing upper row of blocks in three storey building tests by [16];
2) From the side views of Figures 8 - 11, it can be observed that the deformation is different for both models with and without the gravity load. Models without the gravity load behave as cantilevers, while models with gravity load act as having rotation and vertical displacement restricted on column ends;
3) Models with gravity load develop higher initial stiffness and ultimate force than the model without gravity load (Fig.5). In each case, all models developed the same initial stiffness, i.e. not influenced by the infill nor the openings. Same initial stiffness by comparing FI and CW specimen was also found by [17]. Furthermore, the ultimate force for both cases was not influenced by the infill nor the openings. Also, in studies by [17], [18], openings did not influence the ultimate force;
4) The effects of openings is negligible in the case of models without gravity load (Fig.5b). Yet, in the case of models with gravity load, the influence is distinguishable only at post peak behavior. There, FI model has the strongest response and BF model lowest. The models with openings are somewhere in between BF and FI curves. Furthermore, the FI model did not fail at maximal drift ratio while models with openings failed at approximately the same drift ratio as BF model. Reduction of deformation capability was observed by [17] as well;
5) In comparison with infill, for both cases frame attained the greatest amount of damage in regards to cracks (Fig.6&7) and accumulation of stress (Fig.8-11). Without gravity load, models developed plastic hinges at the bottom of the column (Fig.7) while the frames with gravity load develop plastic hinges at the bottom of the column and at column – beam joint;
6) On one hand, the stress in the infill of models without gravity loads are barley observable (Fig.11), and on the other hand the stress in models with gravity load is observable (Fig.10). Hence, in the case of models without gravity load, the arching action did not develop. Yet, in the case of models with gravity load, a two hinge arching action can be noticed. Two hinged arching action happens as the frame translates, the infill clamps at opposite ends and forms compression truss (not arch). The two hinged arching action was also observed on dynamic tests by [15];
7) The difference in displacements between the infill and the frame (Fig.4) is not noticeable, hence, frame and infill behave as single unit. Negligible relative displacements between frame and infill were also found by [19];
8) Block rows started to separate at the lower half of the infill in both cases of loading (Fig.10&11). The separation of rows was also observed on small scale testings of walls subjected to 4 – point bending with load parallel to bedjoints.

References

[1] M. Di Domenico, P. Ricci, and G. M. Verderame, "Experimental Assessment of the Influence of Boundary Conditions on the Out-of-Plane Response of Unreinforced Masonry Infill Walls," *J. Earthq. Eng.*, pp. 1–39, Apr. 2018.

[2] A. Furtado, H. Rodrigues, A. Arêde, and H. Varum, "Experimental Characterization of the In-plane and Out-of-Plane Behaviour of Infill Masonry Walls," *Procedia Eng.*, vol. 114, pp. 862–869, 2015.

[3] P. G. Asteris, L. Cavaleri, F. Di Trapani, and A. K. Tsaris, "Numerical modelling of out-of-plane response of infilled frames: State of the art and future challenges for the equivalent strut macromodels," *Engineering Structures*. 2017.

[4] R. Flanagan and R. Bennett, "Bidirectional behavior of structural clay tile infilled frames," *J. Struct. Eng.*, vol. 125, no. 1985, pp. 236–244, 1999.

[5] R. Henderson, W. Jones, E. Burdette, and M. Porter, "The effect of prior out-of-plane damage on the in-plane behavior of unreinforced masonry infilled frames," in *Fourth DOE Natural Phenomena Hazards Mitigation Conference*, 1993, p. 18.

[6] E. L. McDowell, K. E. McKee, and E. Sevin, "Arching Action Theory of Masonry Walls," *J. Struct. Div.*, vol. 82, no. 2, pp. 1–8, 1956.

[7] A. Furtado, H. Rodrigues, A. Arêde, and H. Varum, "Effect of the Panel Width Support and Columns Axial Load on the Infill Masonry Walls Out-Of-Plane Behavior," *J. Earthq. Eng.*, pp. 1–29, Mar. 2018.

[8] Cervenka Consulting, "ATENA for Non-Linear Finite Element Analysis of Reinforced Concrete Structures." Červenka Consulting s.r.o., Prague, 2015.

[9] D. Penava, V. Sigmund, and I. Kožar, "Validation of a simplified micromodel for analysis of infilled RC frames exposed to cyclic lateral loads," *Bull. Earthq. Eng.*, vol. 14, no. 10, pp. 2779–2804, Oct. 2016.

[10] V. Sigmund and D. Penava, "Influence of openings, with and without confinement, on cyclic response of infilled r-c frames — an experimental study," *J. Earthq. Eng.*, vol. 18, no. November, pp. 113–146, 2014.

[11] CEN, *Methods of Test for Masonry - Part 2: Determination of Flexural Strength (EN 1052-2:1999)*. Brussels: European Committee for Standardization, 1999.

[12] V. Cervenka, L. Jendele, and J. Cervenka, *ATENA Program Documentation Part 1 Theory*. Prague: Cervenka Consulting Ltd., 2012.

[13] F. Anić, D. Penava, and V. Sarhosis, "Development of a three-dimensional computational model for the in-plane and out-of-plane analysis of masonry-infilled reinforced concrete frames," in *6th International Conference on Computational Methods in Structural Dynamics and Earthquake Engineering*, 2017.

[14] ATC-43, "FEMA 306. EVALUATION OF EARTHQUAKE DAMAGED CONCRETE AND MASONRY WALL BUILDINGS. Basic Procedures Manual," 1998.

[15] M. Liu, Y. Cheng, and X. Liu, "Shaking table test on out-of-plane stability of infill masonry wall," *Trans. Tianjin Univ.*, vol. 17, no. 2, pp. 125–131, Apr. 2011.

[16] D. Penava and V. Sigmund, "Out-of-plane behaviour of framed-masonry walls with opening as a result of shaking table tests," *16th World Conf. Earthq. Eng. 16WCEE 2017*, pp. 1–8, 2017.

[17] F. Akhoundi, G. Vasconcelos, P. Lourenco, and L. Silva, "Out-of-plane response of masonry infilled RC frames : Effect of workmanship and opening," in *16th International Brick and Block Masonry Conference*, 2016, pp. 1147–1154.

[18] J. L. Dawe and C. K. Seah, "Out-of-plane resistance of concrete masonry infilled panels," *Can. J. Civ. Eng.*, vol. 16, no. 6, pp. 854–864, Dec. 1989.

[19] J. J. Fowler, "Analysis of dynamic testing performed on structural clay tile infilled frames," 1994.

5 Supplemental

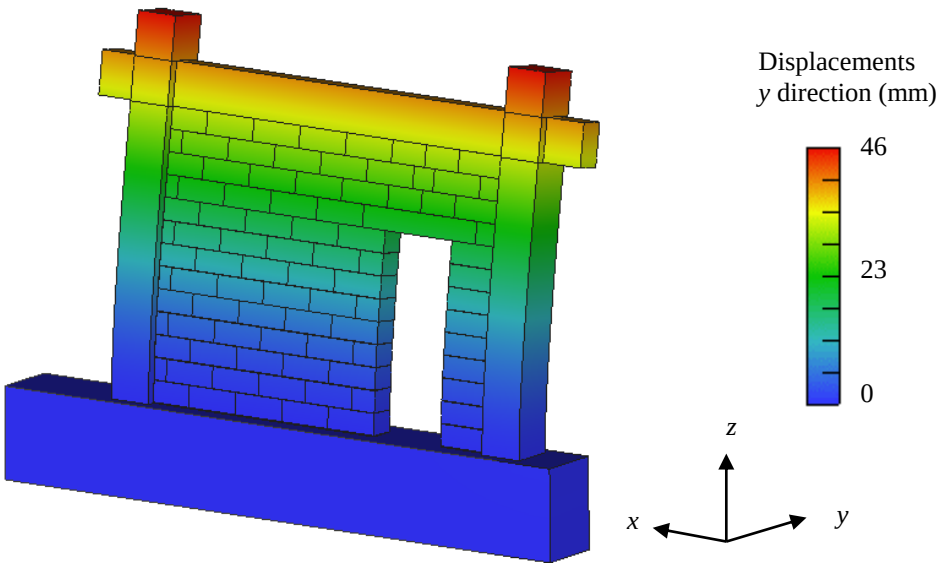

Figure 4: Displacements on ED example of model without gravity load (deformation display enlargement × 5)

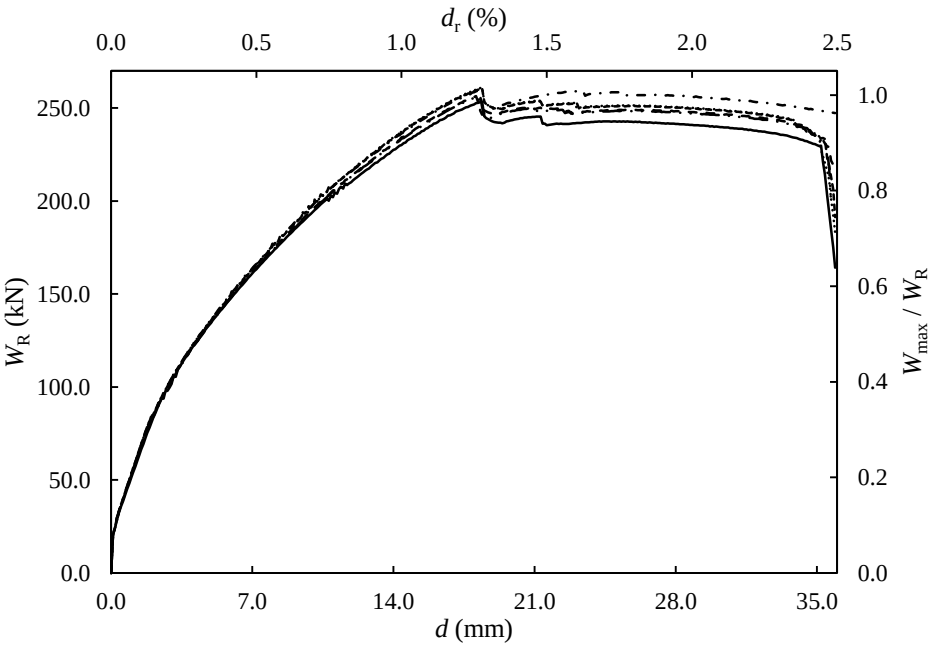

a) With gravity load

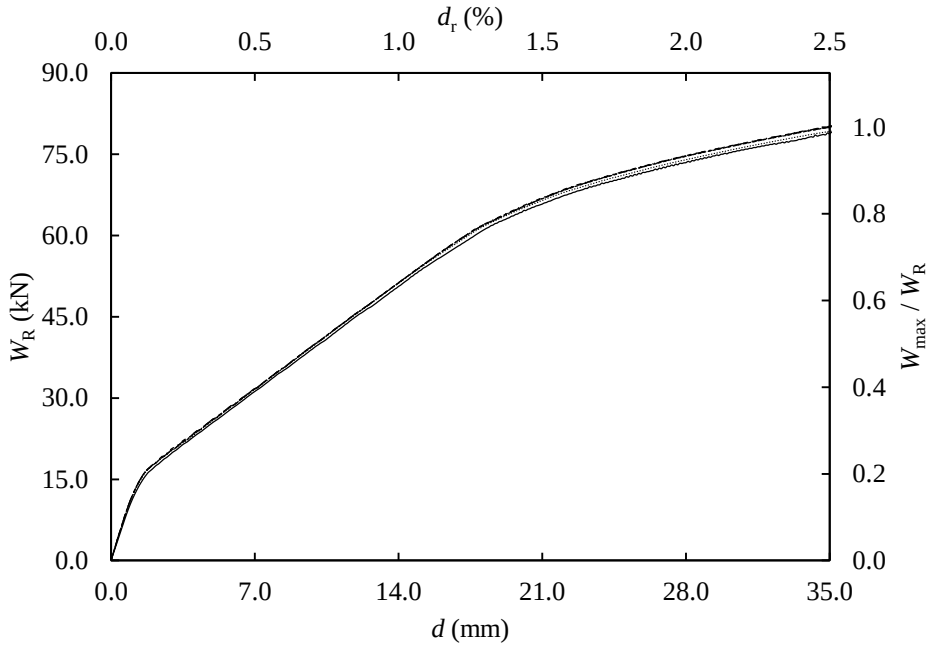

a) Without gravity load

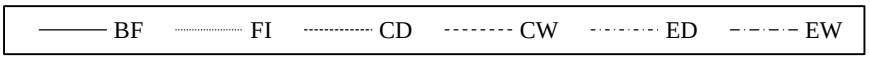

Figure 5: Force vs. displacement diagram

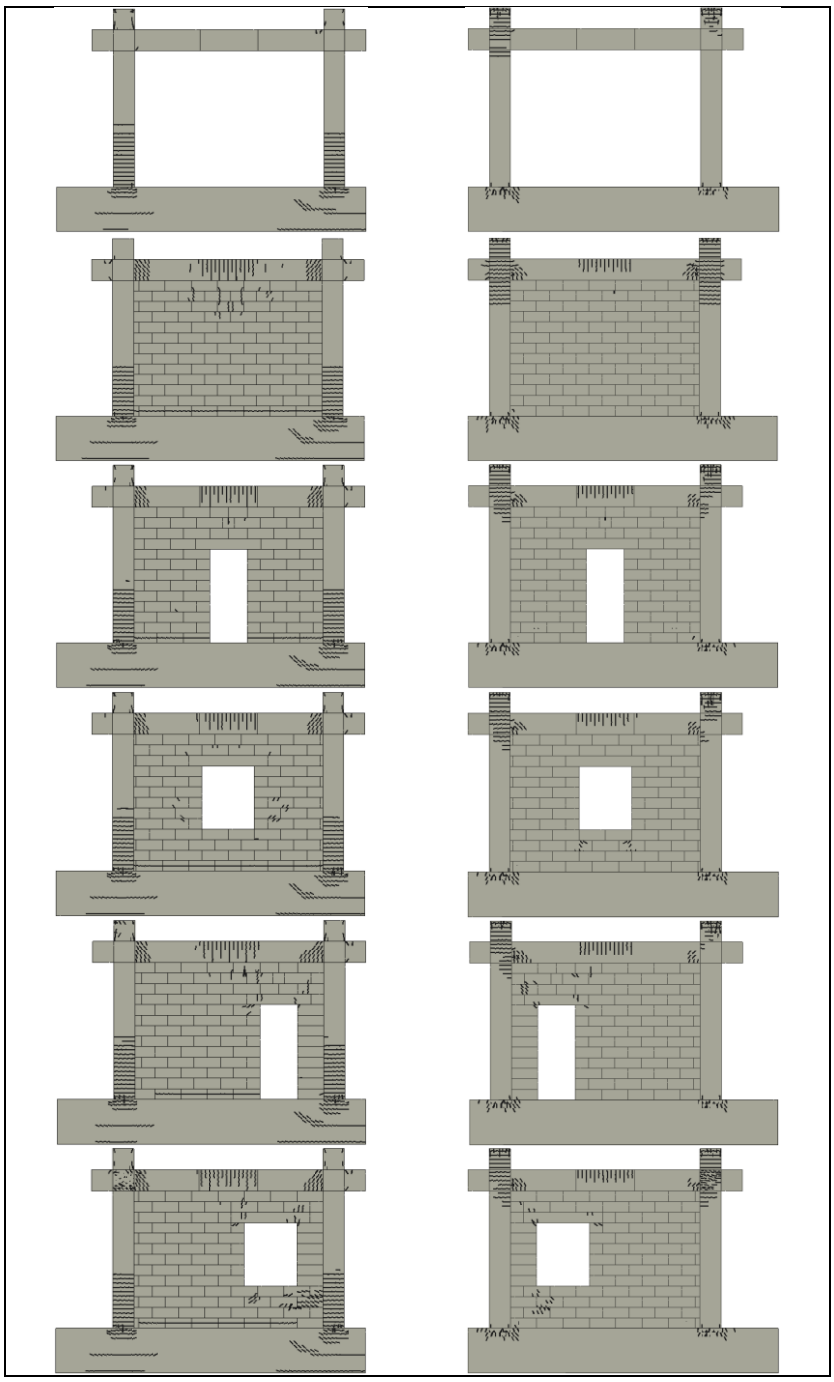

Min crack width = 0.01 mm, Shift cracks outwards ×1, Crack width multiplier × 1, Deformation ×1

Figure 6: Crack patterns maximum drift ratio d_r (left front, right back view), with gravity load

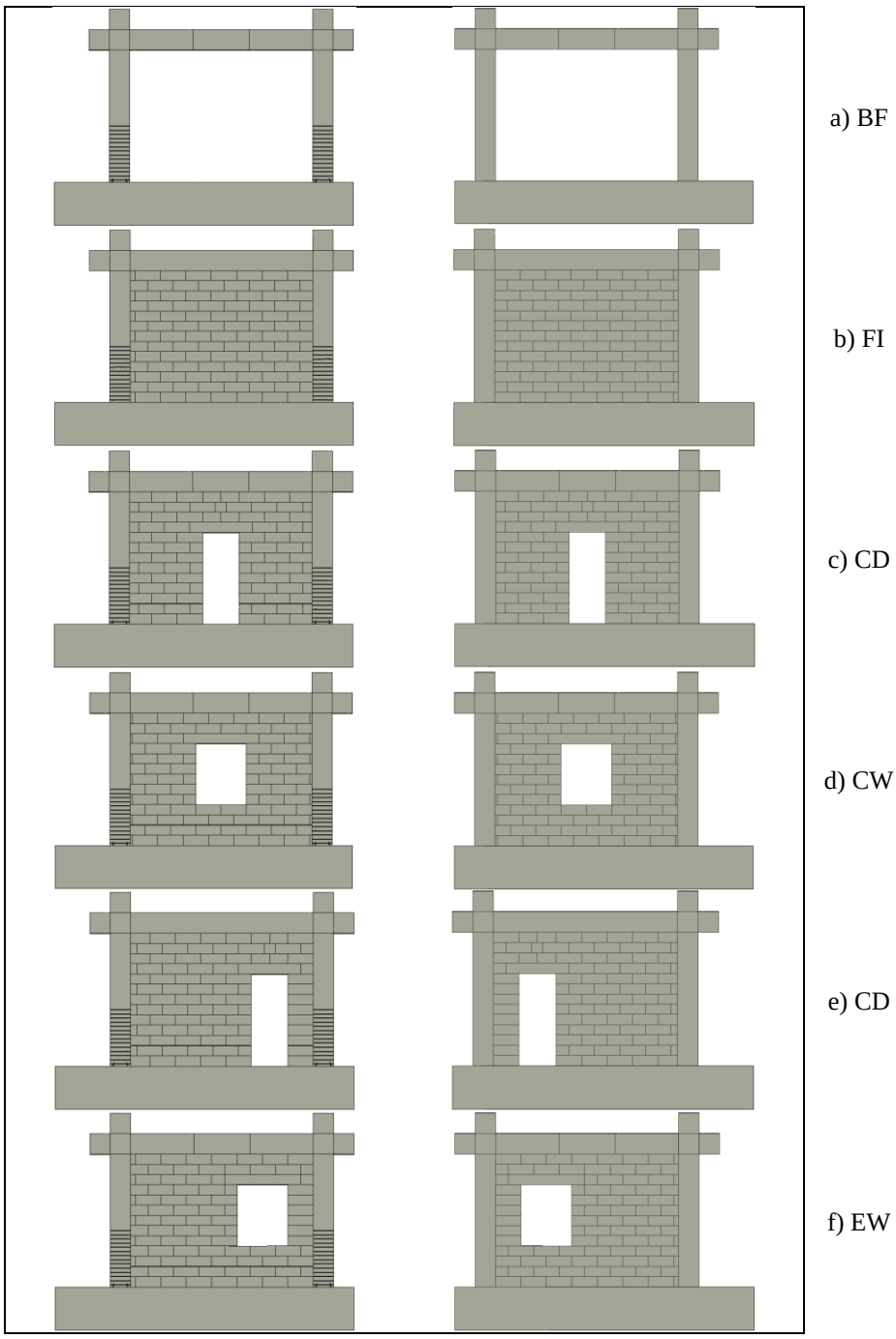

Min crack width = 0.01 mm, Shift cracks outwards ×1, Crack width multiplier × 1, Deformation ×1

Figure 7: Crack patterns maximum drift ratio d_r (left front, right back view), no gravity load

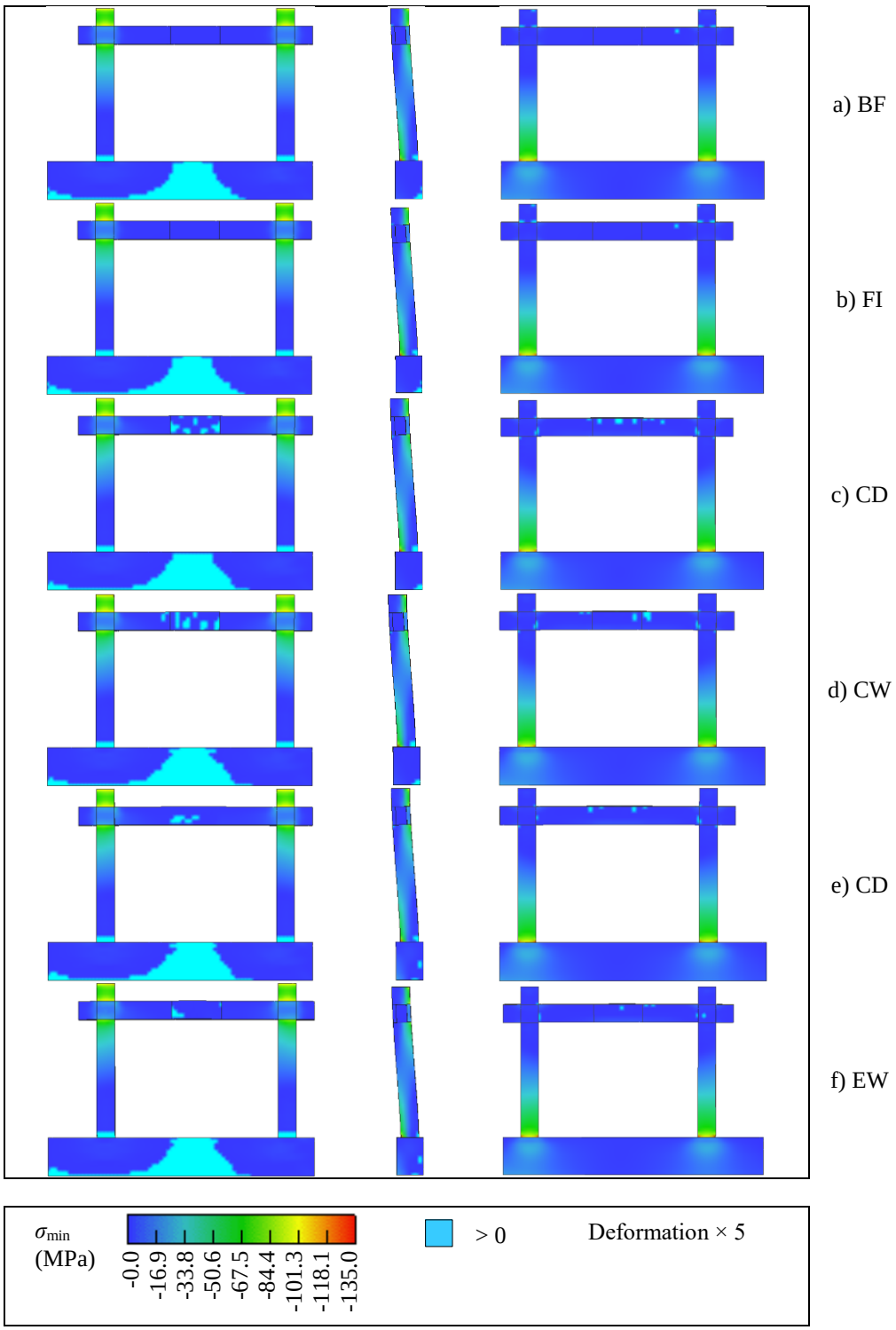

Figure 8: Min. principal stress of the frame at max. force W (left front, right back view), with gravity load

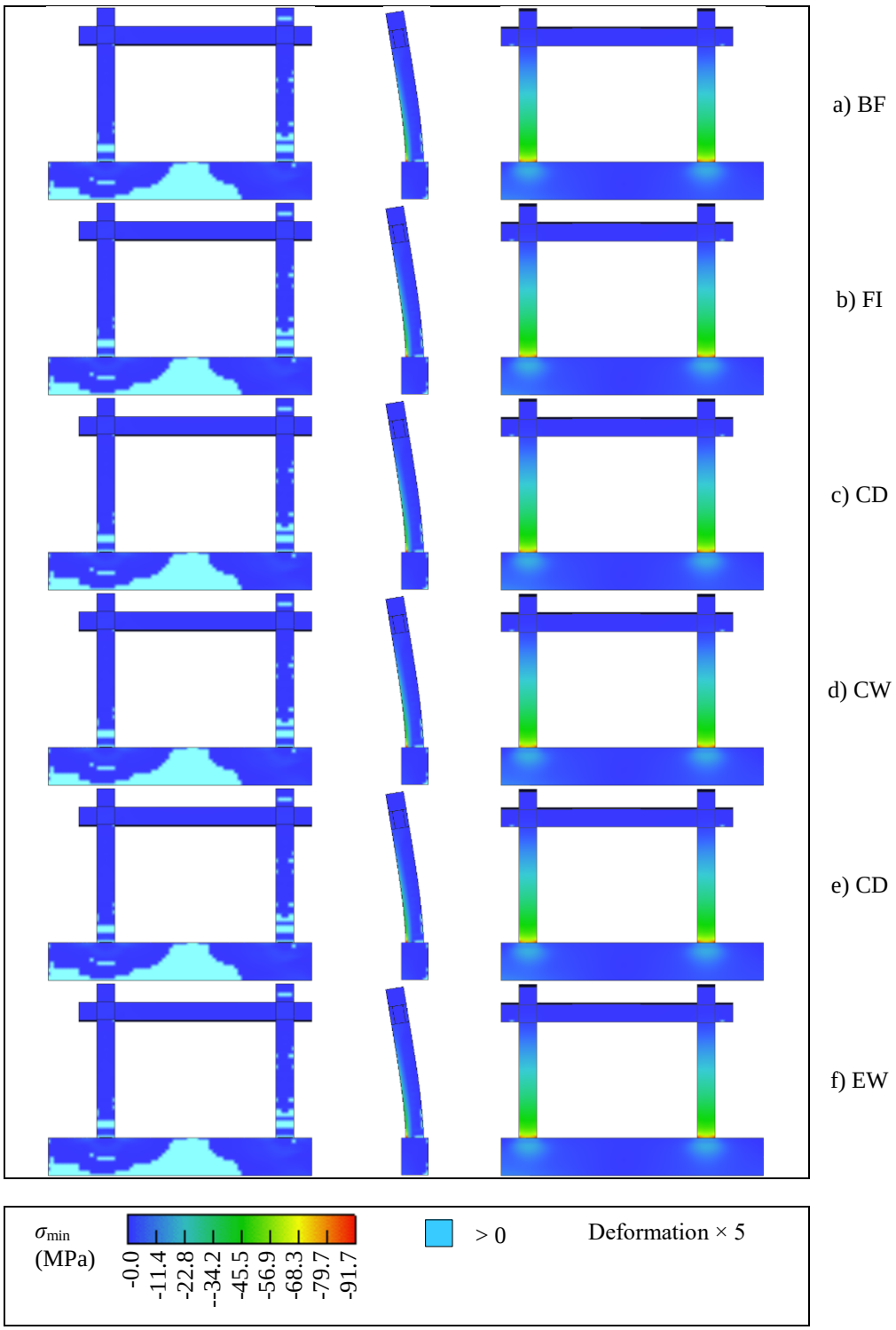

Figure 9: Min. principal stress of the frame at max. force W (left front, right back view), without gravity load

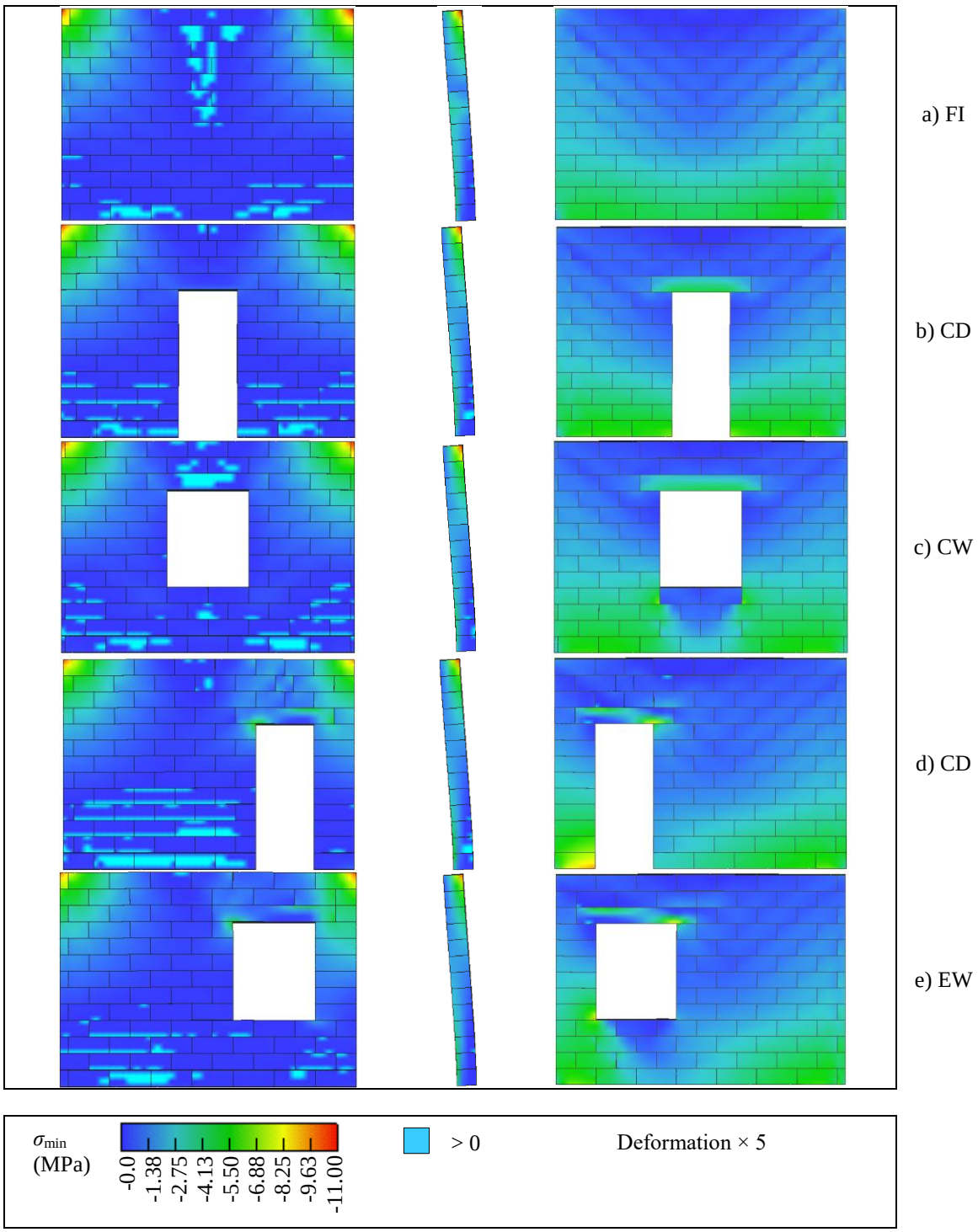

Figure 10: Min. principal stress in infill at max. force *W* (left front, right back view), with gravity load

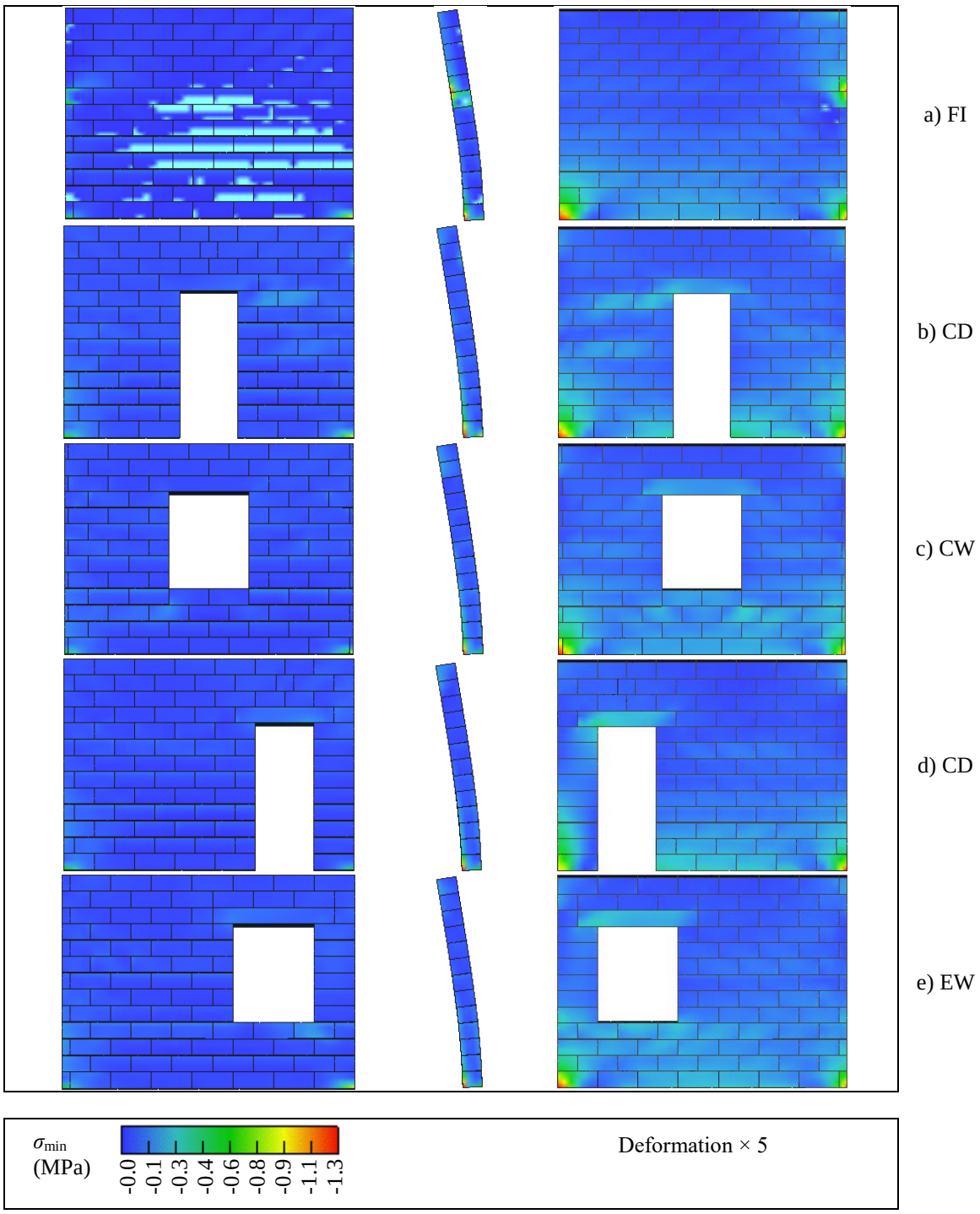

Figure 11: Min. principal stress in infill at max. force *W* (left front, right back view), without gravity load